PLAUSIBLE MODELS OF THE SICKLE HEMOGLOBIN FIBER BASED ON X-RAY DIFFRACTION DATA

BEATRICE MAGDOFF-FAIRCHILD AND LAWRENCE S. ROSEN
Hematology Division, Medical Service St. Luke's-Roosevelt Hospital Center, and Department of Medicine, Columbia University College of Physicians and Surgeons, New York, New York 10025

INTRODUCTION

In sickle cell hemoglobin (Hb S) val replaces glu at the two $\beta 6$ positions of the molecule. This substitution markedly decreases the solubility of the molecule in its unliganded conformation. Polymerization ensues and the aggregates form elongated fibers that distort the shape of the red blood cells into sickled and other bizarre forms. The attendant changes in the viscoelastic properties of the red blood cells are related to the pathogenesis of sickle cell disease. Inhibition of the self-assembly of deoxygenated hemoglobin molecules into fibers would alleviate the symptoms. This could be achieved with stereospecific antisickling agents, whose design would be based on knowledge of the intermolecular contacts that stabilize the helical fiber. Information about the sickle fiber structure could also lead to an understanding of the self-assembly of other biological molecules.

The basic structural unit, or protofilament, of the fiber was determined from the striking similarities between the fiber diffraction pattern and a rotation diagram of the deoxygenated Hb S crystals (Fig. 1). In the crystal, the two molecules of the asymmetric unit are related by a noncrystal lographic pseudo-twofold screw axis parallel to the *a* axis (2). The pair repeats at intervals of 63 Å along the crystallographic *a* axis, or equivalently the fiber axis, forming a double strand in both the crystal and fiber. The molecular *x* axes within these protofilaments enclose an angle of 10° with the crystallographic *a* axis. The close relationship of the molecular orientation and packing in both phases is further demonstrated by the transition of the fiber into the crystalline phase (1, 3).

The architectural features of the fiber were derived from image reconstruction of electron micrographs (4). The fiber comprises 14 molecular strands which exhibit a pseudohexagonal arrangement in projection. These strands have been paired into seven protofilaments, each of which resembles the double strands of the crystal structure (4). The seven protofilaments are derived from two asymmetric units of three-and-one-half protofilaments that are related by a twofold screw axis parallel to the fiber axis. The choice as to which of the adjacent single strands pair to form a protofilament was based on the pattern of loss of filament pairs in partially disassembled fibers (4).

The combined information about the basic structural unit of the fiber, and the fiber architecture provides a means of refining the structure derived from image reconstruction of electron micrographs, and of exploring other plausible models. Two types of models were examined. The first, based on the surface lattice of the reconstruction, utilizes different patterns for the pairing of single strands. The second considers an arrangement of protofilaments similar to the arrangement in the crystal structure. The acceptance of a particular model depends on the degree of correspondence of its transform to the observed fiber diffraction data.

The strategy of refinement of models, based on the reconstructed image (4) or on the crystal structure (1, 8), was to translate one or more protofilaments of the asymmetric unit independently, along the fiber axis, with respect to a reference strand. Throughout these procedures, the double strand configuration remained invariant. Its stabilization depends primarily on the contacts between the substituted $\beta 6$ of one molecule and hydrophobic residues $\beta 85$ phe and $\beta 88$ leu of its neighbor in the adjacent strand (6). Changes in protofilament juxtaposition, however, occur. This is demonstrated by the differences in the separation between the two asymmetric units, along the *a*-axis, in the unit cells of two monoclinic structures (7, 8). In a third crystal form, the triclinic unit cell comprises only one aymmetric unit that forms one protofilament (9). In contrast to the monoclinic case, where the two asymmetric units are of opposite polarity, in the triclinic crystal, the asymmetric unit are all of the same polarity. These and other patterns of protofilament juxtaposition could occur in the fiber and would suggest that several stable polymorphic fiber structures may exist.

RESULTS

Model Based on Electron Microscopy

A search was instituted to determine whether any polymorphic structures other than the corrected, reconstructed image could give an adequate description of the fiber. Prior to such procedures, the positions of molecular centers, as shown in the surface lattice (4), required readjustment because some intermolecular distances were untenably short (5). Moreover, the separation between neighboring molcules in adjacent strands of certain protofilaments differed by as much as 12 Å from the half molecular diameter found in the crystal structure. To eliminate interpenetration, the molecular positions in the projection were shifted; the axial separations between molecules in neighboring strands of a protofilament were adjusted to half a molecular diameter. The major features of the projection were preserved and the protofilament structure corresponded to that in the crystal.

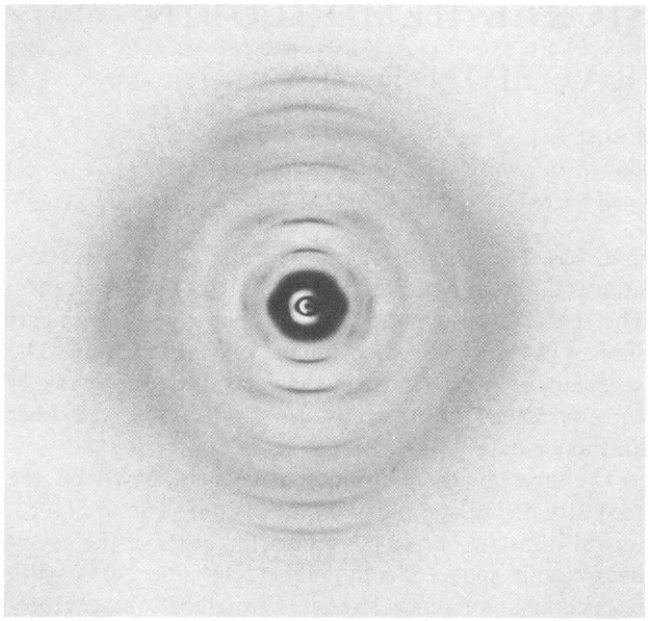

FIGURE 1 X-ray fiber diffraction pattern. The polymers were obtained from high concentration of deoxygenated Hb S. The layer line spacing is $(64\ \text{Å})^{-1}$.

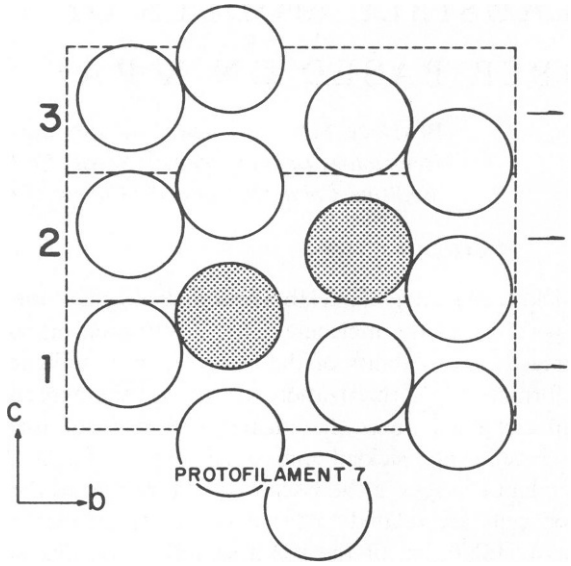

FIGURE 2 A projection down the *a*-axis of the crystal structure of deoxygenated Hb S. The three unit cells (1, 2, and 3) are demarcated with broken lines. Molecules are shown as circles. Each cell contains two protofilaments, related by a local twofold screw axis parallel to *b*. A seventh, isolated protofilament, has been added to the six double filaments in the three unit cells to complete the crystal-based fiber model. Molecules shown in contact form protofilaments. A molecular radius of 23 Å was chosen for this projection to eliminate overlap in the drawing. The two molecules corresponding to the central protofilament of the reconstruction are shaded. In our crystal-based model, these adjacent strands are not in the same protofilament. Each of these shaded molecules is associated with another molecule in a neighboring strand to form two protofilaments.

The transforms of 5,800 models, generated by systematic shifts of the three protofilaments of the asymmetric unit in steps of 3.5 Å parallel to the fiber axis, were calculated and compared with the x-ray diffraction data of 15 Å resolution (5). The comparison which gave the lowest residual was for a model that differed from the reconstructed image. Application of a statistical criterion (10) to the ratios of residuals permitted the rejection of the reconstructed image in favor of this model with a confidence level of 99.5%. It is of interest that at the resolution of the electron micrographs, the residuals of both the reconstructed image and the "best" structure are the same.

Another mode of associating strands into protofilaments (5), consistent with the surface lattice and the pattern of filament loss (4), was explored. Two structures with this alternate pairing pattern gave equivalent minimal residuals. These models have about the same residuals as the residual for the structure based on the initial pairing scheme that was accepted with 99.5% certainty. The reconstructed image, however, could not be rejected with the same degree of confidence as before because of the decreased number of degrees of freedom associated with these models for the determination of statistical significance. At 15 Å resolution, any of these three models may serve as an equally acceptable representation of the fiber structure.

Models Based on Crystal Structures

The resemblance of the projection of the reconstructed image to the packing in the crystallographic *bc* net suggests another possible model of the fiber. The difference between this model and the "best" ones derived from the reconstructed image resides primarily in the manner in which single strands pair into protofilaments. In this model, six protofilaments are packed and oriented as shown in projection (Fig. 2). A seventh is added to complete the fiber. This crystal-based fiber structure does not possess a twofold screw axis as does the model based on the reconstructed image. Its only symmetry elements are local twofold screw axes along *b* that relate the two protofilaments within each subcell.

A search for crystal-based models with minimal residuals employs three variable parameters that specify the axial displacement of each of the subcells with respect to the stationary seventh protofilament. Three additional parameters define whether the two protofilaments in each subcell are related as they are in form I or II structures. In form I, the separation along the *a*-axis between protofilaments related by the twofold screw axis is approximately $a/4$ while in form II, both protofilaments are in register (8). More than 46,000 transforms of independent models were examined. These models comprised a complete range of axial translations, in steps of 3.5 Å, for each of the subcells. They encompass the eight ways of arranging forms I and II in three subcells. To reduce the enormous

TABLE I

RELATIVE UNIT CELL HEIGHTS ALONG THE FIBER AXIS (IN A) OF THE THREE 'BEST' CRYSTAL-BASED MODELS

	Models		
Unit cell	A	B	C
1	46.1	46.1	14.1
2	14.1	46.1	46.1
3	46.1	14.1	14.1

computational requirements of these searches for minimal residuals, transforms of each of these models were computed with algorithms related to the one used for calculating the transforms of models based on the reconstructed image (5). With this simplification, the structure factors had to be calculated only once for an initial model.

Calculations show that there are three closely related models with minimal residuals of ~17% and 11% for the second and third layer lines of the fiber diffraction pattern. All of these models contain form II structure in each of the three subcells. The heights along the fiber axis of each unit cell with respect to the seventh protofilament are given in Table I.

Model *B* is of particular interest. The heights of the first and second subcells are the same with respect to protofilament 7. Consequently, the central filaments residing in these two subcells (shaded circles, Fig. 2) are separated by half a molecular diameter along the fiber axis. Such a separation is a reliable feature of the reconstructed image (4). The two central strands in Model *B* belong to separate protofilaments and are of opposite polarity. In the reconstructed image, these strands are in the same protofilament and of the same polarity.

DISCUSSION

We have identified six structures based on diffraction data of 15 Å resolution whose residuals are lower than the residual of the reconstructed image. Three of the models were derived directly from the reconstructed image, and are statistically more likely to represent the fiber structure than the reconstructed image. The remaining three structures are crystal based and were selected from among 46,000 models on the basis of their minimal residuals. Only one of these three satisfies the constraint imposed by the reconstructed image, i.e. the two central strands be separated by half a molecular diameter along the fiber axis. The residuals of all three are about the same as the residuals of the three models in which the pairing of strands was taken initially from the surface lattice of the reconstructed image.

These results do not allow the selection of one of the six models as the most accurate representation of the fiber structure. Crystal-based models, however, are preferable to those derived from pairing schemes based on the surface lattice of the reconstructed image. Fibers coalesce to form bundles (11–13). Helices may unwind and crystallization would then proceed. Such a pattern of change in the crystal-derived model, leading to a phase transition, would be energetically favorable compared with the complex rearrangement of protofilaments required for the models based on image reconstruction.

This work was supported by National Institutes of Health grants HL 23984 and HL 28381.

REFERENCES

1. Magdoff-Fairchild, B., and C. C. Chiu. 1979. X-ray diffraction studies of fibers and crystals of deoxygenated sickle cell hemoglobin. *Proc. Natl. Acad. Sci. USA.* 76:223–226.
2. Wishner, B., K. B. Ward, E. E. Lattman, and W. E. Love. 1975. The crystal structure of sickle-cell deoxyhemoglobin. *J. Mol. Biol.* 98:161–178.
3. Hofrichter, J., P. D. Ross, and W. A. Eaton. 1976. A physical description of hemoglobin S gelation. *In* Proceedings of the Symposium on Molecular and Cellular Aspects of Sickle Cell Disease. Hercules, J. I., G. L. Cottram, M. R. Waterman, and A. N. Schechter, editors. DHEW Pub. No. (NIH) 76-1007. 185–222.
4. Dykes, G., R. H. Crepeau, and S. J. Edelstein. 1979. Three dimensional reconstruction of the 14-filament fibers of Hb S. *J. Mol. Biol.* 130:451–472.
5. Rosen, L. S., and B. Magdoff-Fairchild. 1985. X-ray diffraction studies of 14-filament models of deoxygenated Hb S fibers. I. Models based on electron micrograph reconstructions. *J. Mol. Biol.* 183:565–574.
6. Wishner, B. C., J. C. Hanson, W. M. Ringle, and W. E. Love. 1976. Crystal structure of sickle-cell deoxyhemoglobin. *In* Proceedings of the Symposium on Molecular and Cellular Aspects of Sickle Cell Disease. J. I. Hercules, G. L. Cottram, M. R. Waterman, and A. N. Schechter, editors. DHEW Pub. No. (NIH) 76-1007. 1–29.
7. Chiu, C. C., and B. Magdoff-Fairchild. 1980. Deoxygenated sickle hemoglobin. Phase transformation from fiber to a new monoclinic crystalline form. *J. Mol. Biol.* 136:455–459.
8. Rosen, L. S., and B. Magdoff-Fairchild. 1982. Molecular packing in a second monoclinic crystal of deoxygenated sickle hemoglobin. *J. Mol. Biol.* 157:181–189.
9. Magdoff-Fairchild, B., L. S. Rosen, and C. C. Chiu. 1982. Triclinic crystals associated with fibers of deoxygenated sickle hemoglobin. *EMBO J.* 1:121–126.
10. Hamilton, W. 1965. Significance tests on the crystallographic R factor. *Acta Cryst.* 18:502–510.
11. Wellems, T. E., R. J. Vassar, and R. Josephs. 1981. Polymorphic assemblies of double strands of sickle cell hemoglobin. *J. Mol. Biol.* 153:1011–1026.
12. Vassar, R. J., M. J. Potel, and R. Josephs. 1982. Studies of the fiber to crystal transition of sickle cell hemoglobin in acidic polyethylene glycol. *J. Mol. Biol.* 157:395–412.
13. Potel, M. J., T. E. Wellems, R. J. Vassar, B. Deer, and R. Josephs. 1984. Macrofiber structure and the dynamics of sickle cell hemoglobin crystallization. *J. Mol. Biol.* 177:819–839.